



Development of high-precision micro-coordinate measuring machine: Multi-probe measurement system for measuring yaw and straightness motion error of XY linear stage

Ping Yang^a, Tomohiko Takamura^a, Satoru Takahashi^a, Kiyoshi Takamasu^{a,*}, Osamu Sato^b, Sonko Osawa^b, Toshiyuki Takatsuji^b

^a Department of Precision Engineering, The University of Tokyo, Hongo 7-3-1, Bunkyo-ku, Tokyo 113-8656, Japan

^b National Metrology Institute of Japan, National Institute of Advanced Industrial Science and Technology, Umezono 1-1-1, Tsukuba, Ibaraki 305-8563, Japan

ARTICLE INFO

Article history:

Received 2 July 2010

Received in revised form 7 December 2010

Accepted 6 January 2011

Available online 28 January 2011

Keywords:

Micro-CMM

Multi-probe measurement method

Uncertainty

Motion errors

XY stage

ABSTRACT

Today, with the development of microsystem technologies, demands for three-dimensional (3D) metrologies for microsystem components have increased. High-accuracy micro-coordinate measuring machines (micro-CMMs) have been developed to satisfy these demands. A high-precision micro-CMM (M-CMM) is currently under development at the National Metrology Institute of Japan in the National Institute of Advanced Industrial Science and Technology (AIST), in collaboration with the University of Tokyo. The moving volume of the M-CMM is 160 mm × 160 mm × 100 mm (XYZ), and our aim is to achieve 50-nm measurement uncertainty with a measuring volume of 30 mm × 30 mm × 10 mm (XYZ). The M-CMM configuration comprises three main parts: a cross XY-axis, a separate Z-axis, and a changeable probe unit. We have designed a multi-probe measurement system to evaluate the motion accuracy of each stage of the M-CMM. In the measurement system, one autocollimator measures the yaw error of the moving stage, while two laser interferometers simultaneously probe the surface of a reference bar mirror that is fixed on top of an XY linear stage. The straightness motion error and the reference bar mirror profile are reconstructed by the application of simultaneous linear equations and least-squares methods. In this paper, we have discussed the simulation results of the uncertainty value of the multi-probe measurement method using different intervals and standard deviations of the laser interferometers. We also conducted pre-experiments of the multi-probe measurement method for evaluating the motion errors of the XY linear stage based on a stepper motor system. The results from the pre-experiment verify that the multi-probe measurement method performs the yaw and straightness motion error measurement extremely well. Comparisons with the simulation results demonstrate that the multi-probe measurement method can also measure the reference bar mirror profile with a small standard deviation of 10 nm.

© 2011 Elsevier Inc. All rights reserved.

1. Introduction

In recent times, miniaturization and modularization of microsystem technologies have attracted considerable attention as methods to improve the manufacture efficiencies of small size products with high accuracy. Further, as the result, it has become increasingly important to be able to perform three-dimensional (3D) measurements of nano and microstructures with uncertainties within 0.1 μm. However, conventional measuring methods cannot meet these requirements because the measurement scales of conventional coordinate measuring machines (CMMs) are usually limited to several tens of millimeters or more, which is not suit-

able for measuring small parts of the order of submillimeters or even submicrometers. In addition, conventional CMMs lack good 3D measurement uncertainty levels and are often not supplied with the proper probing systems in many applications [1]. Therefore, micro-CMMs equipped with special micro-probe systems for 3D metrology having high-aspect-ratio micro parts are currently being developed to satisfy the described requirements. Some researches on micro-CMMs are discussed in the following paragraph.

Isara (IBS Precision Engineering) is an ultra-precision CMM that is now available in the market; it comprises a moving product table and a metrology frame with thermal shielding on which three laser sources are mounted [2]. The F25 micro-CMM (Carl Zeiss) is another commercially available product. Further, the National Physical Laboratory (NPL) is currently conducting researches into reducing the size of the probing sphere so that the measurements of even smaller structures can be performed. The Physikalisch-

* Corresponding author. Tel.: +81 035 841 6450; fax: +81 035 841 8554.

E-mail address: takamasu@pe.t.u-tokyo.ac.jp (K. Takamasu).

Table 1
Specifications of micro-CMMs.

Micro-CMMs	Range-XYZ (mm)	Uncertainty (nm)
Isara	100 × 100 × 40	30
F25	100 × 100 × 100	≤100
M-NanoCoord	200 × 200 × 100	200
M-CMM	160 × 160 × 100	50 (target)

Technische Bundesanstalt (PTB) is working along with Carl Zeiss in the field of 3D micrometrology research. M-NanoCoord designed by Mitutoyo is a flexible 3D vision measuring machine using the UMAP103 probe system [3,4]. The specifications of these products are listed in Table 1.

We have developed a novel high-precision micro-CMM called M-CMM, and a prototype has been constructed at the National Institute of Advanced Industrial Science and Technology (AIST), Japan. In this M-CMM, we are aiming to achieve measurement uncertainty of 50-nm in a measuring volume of 30 mm × 30 mm × 10 mm (XYZ). Since the motion errors of each stage of the M-CMM should be calibrated and compensated in order to develop a high precision M-CMM, we have proposed a multi-probe measurement method and discussed its applications for evaluating the yaw and straightness motion error of each stage.

2. M-CMM configuration

The M-CMM configuration comprises three main parts: a cross XY-axis, a Z-axis, and a probe unit. Each axis has a linear motion stage system that comprises air-bearing sliders, a glass linear scale, a moving table, a driving motor, and related parts. Linear motion stage systems have been successfully employed in precision measurement systems because of the lack of friction in the air-bearing sliders. Further, the area-averaging effect on the guide error leads to high positioning accuracy and low traveling motion errors. In addition, the linear scales feedback the position signal within the range of the nanometer resolution.

There are three special specifications in the M-CMM design. The frame table and main structure of each axis is made of alumina ceramic having high rigidity and low coefficient of thermal expansion (CTE; 7 ppm/K). Further, the base plate of the M-CMM is made of granite having CTE of 5 ppm/K, as shown in Fig. 1. In general, thermal effects are one of the most significant reasons of non-repeatability in measuring machine accuracy. The M-CMM minimizes these effects using the same alumina ceramic materials. Because of this optimized design, when the temperature changes, the main mechanical structures will deform almost in the same

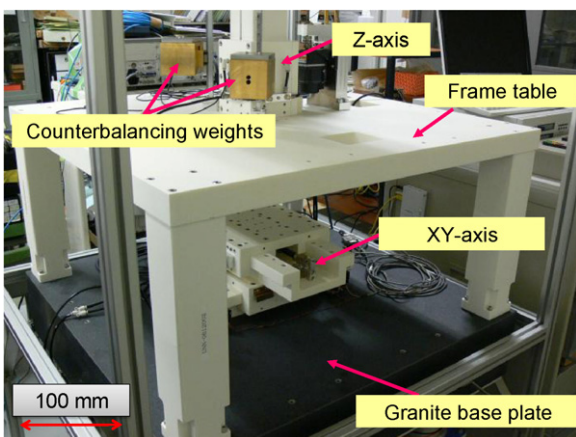


Fig. 1. Main structure of micro-coordinate measuring machine (M-CMM).

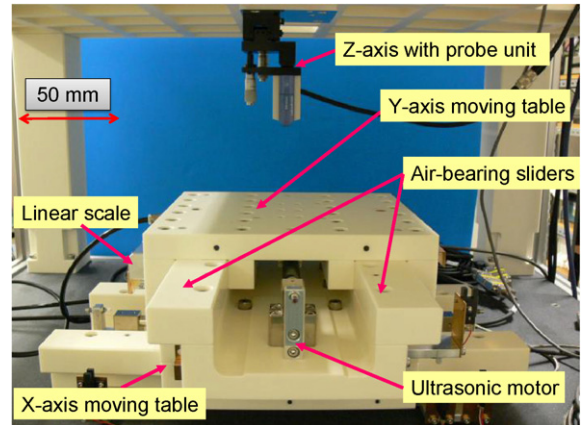


Fig. 2. Structure of XY stage and probe unit.

deviation range. On the other hand, the measurement area is covered with an enclosure to minimize heat inputs from the machine environment (e.g., from operators). Therefore, the M-CMM exhibits good performance in response to temperature changes, and thermal deformations due to the driving heat and temperature changes are significantly reduced. We subsequently divided the XYZ-axis into two mechanical parts: the XY-axis, which is stacked with two linear stages, and the Z-axis, which is separately designed and constructed at the center of the frame table. The primary reason for this division is that the measurement uncertainties of the Z-axis are larger than those of the XY-axis because the sensitivity of the 3D contacting micro-probes in the Z-direction is usually lower than that in the XY plane; this, in turn, is due to the effect of the length of the probe stylus on the horizontal probing direction. Finally, the probe unit has a changeable connector, and hence, the M-CMM can use different types of contacting probe systems and conduct 3D measurements with different levels of uncertainties.

2.1. XY-axis

The XY-axis is a stacking-type mechanism having two linear stages comprising air-bearing sliders, ultrasonic motors (linear motors), moving tables, linear scales, and related parts, as shown in Fig. 2. The XY stage is fixed on a granite base plate. Each stage of the XY-axis is driven by an ultrasonic motor, and its movement is detected by a linear scale mounted on the side of the moving stage. A moving table with a size of 280 mm × 280 mm has sufficient space to perform calibrations and compensations.

2.2. Z-axis

The Z-axis is designed separately and embedded in the center of a frame table built on the base plate, as shown in Figs. 1 and 2. Unlike the traditional CMMs, the Z-axis motion is less affected by the movement of other axes. The Z-axis mechanism consists of a counterbalancing weight, air-bearing sliders, AC servomotor, and related parts. The weight of the Z stage is supported not only by a ball screw connected to the AC motor but also by the counterbalancing weight that is used to control the moment transfer from the ball screw. Thus, the load on the elastic hinge can be reduced. To control the balance in the orthogonal direction, the two counterbalancing weights and ball screw have 120-degree rotational symmetry. The movement range of the Z stage can then reach 100 mm. At the bottom of the Z-axis, there is a changeable connector that allows us to employ different probe systems to perform the measurements.

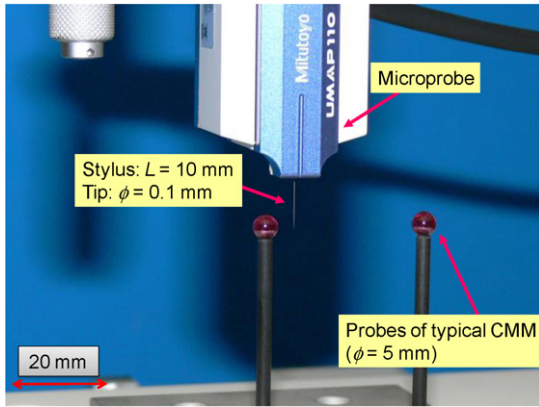


Fig. 3. Probe unit using UMAP 110.

Table 2 Specifications of probe units.

Probe	Stylus length	Repeatability	Tip diameter
Renishaw TP 200	Up to 100 mm	$2\sigma = 0.4 \mu\text{m}$	$\varphi < 1 \text{ mm}$
Mitutoyo UMAP 110	10 mm	$\sigma = 0.15 \mu\text{m}$	100–110 μm
Mitutoyo UMAP 103	2 mm	$\sigma < 0.1 \mu\text{m}$	30 μm

2.3. Probe unit

The probe unit is mounted on the Z-axis, as shown in Fig. 2; it includes a changeable connector that allows the M-CMM to perform 3D measurements with different levels of probing systems. The probe systems that contain Renishaw TP200, Mitutoyo UMAP110, and Mitutoyo UMAP103 will be used to achieve different levels of 3D measurement uncertainties. Fig. 3 shows a probe unit using UMAP 110. The specifications of these probe units are shown in Table 2.

3. Calibration of yaw and straightness motion error using multi-probe method

3.1. Motion degrees of freedom and Abbe error

In a 3D space, any positioning stage has six degrees of freedom (DOFs): three translational errors and three rotational errors. Because of the mechanical design, we cannot satisfy the Abbe principle, and the Abbe error will exist. The Abbe errors are caused by the rotational errors of relative translations between the reference and sensing points; the Abbe offsets are the distances between the reference and sensing points. The Abbe errors are often the most important uncertainty sources in dimensional metrology applications that require measurement uncertainties of only a few nanometers [5–7]. For example, when the Abbe offset H is 10 mm, if we can control the tilt of the X axis, θ , to be 1 μrad , the Abbe error δ in the X direction will reduce to 10 nm (Fig. 4). Therefore, the 6 DOFs of each stage of the M-CMM are very important factors in the development of a high-precision M-CMM.

The motion errors of the M-CMM without any compensation are shown in Table 3. For instance, the Abbe error of the XY-axis

Table 3 Motion errors of M-CMM without compensation.

Axis	Degrees of freedom	Accuracy/range
X,Y	Straightness	Max: 0.5 $\mu\text{m}/160 \text{ mm}$
X,Y	Tilting	Max: 8 $\mu\text{rad}/160 \text{ mm}$
Z	Straightness	Max: 0.3 m/100 mm
Z	Tilting	Max: 5 $\mu\text{rad}/100 \text{ mm}$

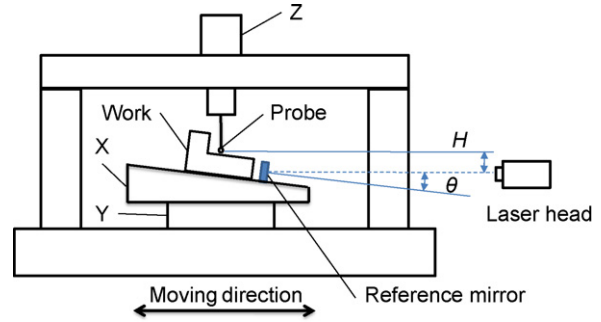


Fig. 4. Illustration of Abbe error after compensation.

can be in the micrometer range. Hence, the motion errors of the XY stage in the M-CMM should be measured and calibrated. In the traditional calibration method, one displacement sensor is used with a high-accuracy reference bar mirror. The accuracy of this method is dependent on the accuracy of the reference mirror because the final measured results include the profile of the reference bar mirror. Hence, an error separation technique employing several displacement probes has been proposed and developed, and other applications using the multi-probe methods have been widely used for realizing precision measurements [8–14]. In our measurement system, we use the multi-probe measurement method to measure the yaw and straightness motion error of each linear stage; the reference bar mirror profile is also reconstructed by the application of the simultaneous linear equations and least-squares methods [13,14].

3.2. Principle of multi-probe method

In the measurement system, one autocollimator measures the yaw error of the stage, while multiple laser interferometers probe the surface of a reference bar mirror fixed on top of the XY-axis. Unlike the case wherein the position sensors are fixed on a moving scanner, the laser interferometers are mounted on stationary housings, as shown in Fig. 5 [15,16]. Let the corresponding laser interferometers and autocollimator outputs be $m_1(n), m_2(n), \dots, m_M(n)$ and $m_a(n)$. They can be expressed as follows:

$$\begin{cases} m_1(n) = f(x_n + 0) + e_s(n) + 0 \cdot e_y(n) + u_1 + b_0 \\ m_2(n) = f(x_n + D_1) + e_s(n) + D_1 \cdot e_y(n) + u_2 + b_0 \\ \vdots \\ m_M(n) = f(x_n + D_M) + e_s(n) + D_M \cdot e_y(n) + u_M + b_0 \\ m_a(n) = e_y(n) + u_a \\ n = 1 \dots N_s \end{cases} \quad (1)$$

Here $f(x_n)$, the reference bar mirror profile; $e_y(n)$ and $e_s(n)$, the yaw and straightness motion error of the moving stage, respectively; D_1 , the interval of the 2nd to the 1st laser interferometer; D_M , the interval of the Mth to the 1st laser interferometer; $N_s = N - d_M$,

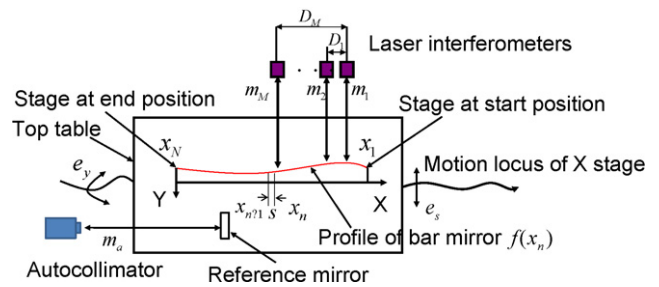


Fig. 5. Principle of multi-probe method.

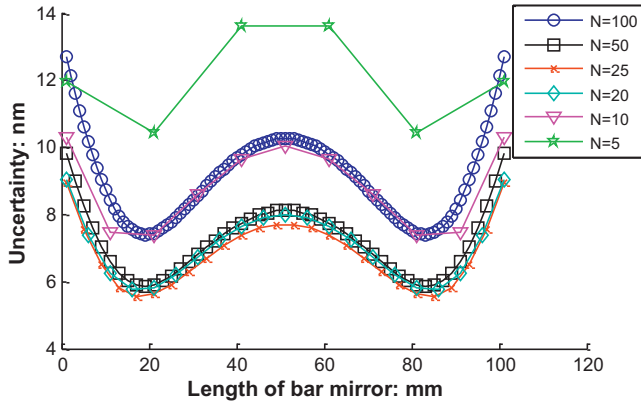


Fig. 6. Relation between the interval of laser interferometers D_1 and the uncertainty of multi-probe method, when $\sigma_1 = \sigma_2 = 1.2$ nm and $\sigma_a = 0.5$ μ rad.

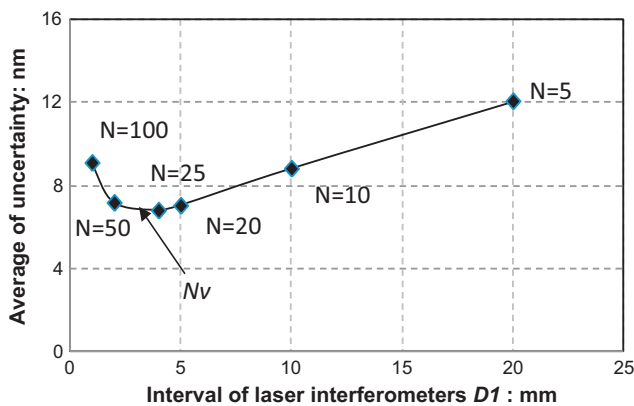


Fig. 7. Relation between the interval of laser interferometers D_1 and the average uncertainty value of multi-probe method, when $\sigma_1 = \sigma_2 = 1.2$ nm and $\sigma_a = 0.5$ μ rad.

Our second condition is $D_1 = s = 10$ nm; here, we use the following values of the standard deviations of the laser interferometers: $\sigma_1 = \sigma_2$: 1.2 nm, 2 nm, 5 nm, 10 nm, and 20 nm. The simulation results are shown in Fig. 8. In this simulation group, N and σ_a are fixed values, and only the standard deviations of the laser interferometers, σ_M , exhibit variations. The simulation results show that the uncertainties increase continuously with σ_M .

By comparing the simulation results of these two groups, we can conclude that the multi-probe measurement method adequately performs the measurements of the yaw and the straightness motion errors with small standard deviations. For instance, when we set $\sigma_1 = \sigma_2 = 1.2$ nm (second condition), the uncertainty value 2σ is

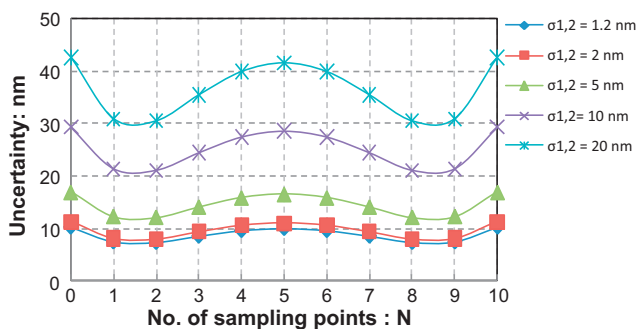


Fig. 8. Relation between the standard deviation values of laser interferometers, σ_M , and the uncertainty of multi-probe method, when $N = 10$ and $\sigma_a = 0.5$ μ rad.

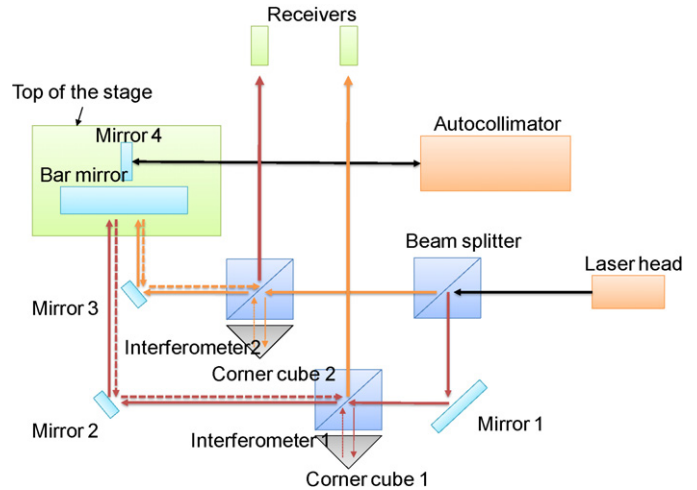


Fig. 9. Block diagram of pre-experiment.

approximately 10 nm (Fig. 6). This is sufficient for us to achieve our aim of 50-nm uncertainty. To verify the performance of the multi-probe measurement method in real applications, we have designed a pre-experiment.

5. Configuration of pre-experiment

The pre-experiment of the multi-probe method has been designed to measure the motion errors of an XY stage based on a stepper motor system. In the pre-experiment, an autocollimator measured the yaw error of the moving stage, and two laser interferometers probed the surface of the reference bar mirror fixed on top of the XY stage. Fig. 9 shows the block diagram of the pre-experiment that consisted of optical reflection devices, an XY stepper motor stage, laser interferometers, receivers, beam splitters, optical reflection mirrors, and an autocollimator. The optical reflection devices that are fixed on top of the XY stage consisted of a reference bar mirror, a housing for the reference bar mirror, and a reference mirror for the autocollimator (mirror 4). The pre-experiment was conducted by two laser interferometers and one autocollimator simultaneously (Fig. 10). The moving direction of the X-axis was from left to right. The valid size of the reference bar mirror is 100 mm \times 30 mm with an accuracy of $\lambda = 632.8$ nm. The sampling length of the reference bar mirror was 100 mm. When $D_1 = s = 10$ nm, the interval of the laser interferometers was identical to the measuring step distance; N was 10, and $N_s = N - D_M$ was 9.

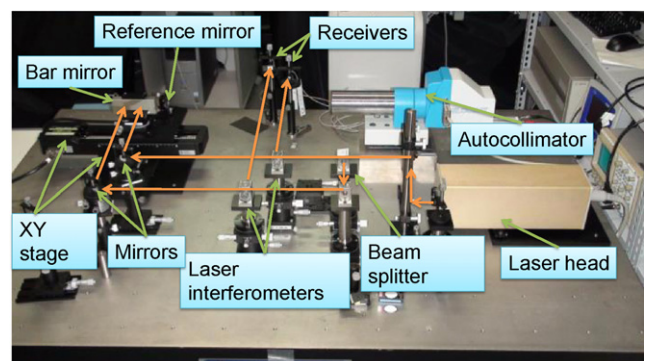


Fig. 10. Main set up of pre-experiment.

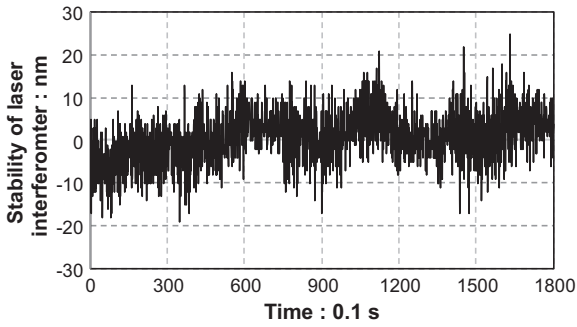


Fig. 11. Stability of laser interferometer.

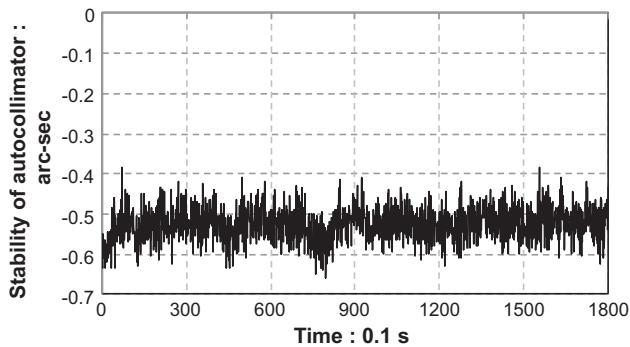


Fig. 12. Stability of autocollimator.

6. Pre-experiment results

In order to verify the standard deviation of each sensor in a real environment, we measured the stabilities of the laser interferometers and autocollimator shown in Figs. 11 and 12, respectively. We found the standard deviations of the laser interferometers and autocollimator to be $\sigma_1 = \sigma_2 = 4$ nm, and $\sigma_a = 0.23 \mu\text{rad}$, respectively, in the pre-experiment. The standard deviations of the laser interferometers in the real environment were larger than the theoretical resolution value of 1.2 nm because the laser interferometers are sensitively affected by the measurement environment and other factors.

The experiment was repeated nine times, and the yaw errors of the X-axis are presented in Fig. 13. The yaw error range is approximately $30 \mu\text{rad}$. The straightness motion errors of the X-axis obtained by the application of the simultaneous equations and least-squares methods are shown in Fig. 14. The straightness motion error range is approximately $\pm 1 \mu\text{m}$. The reconstructed ref-

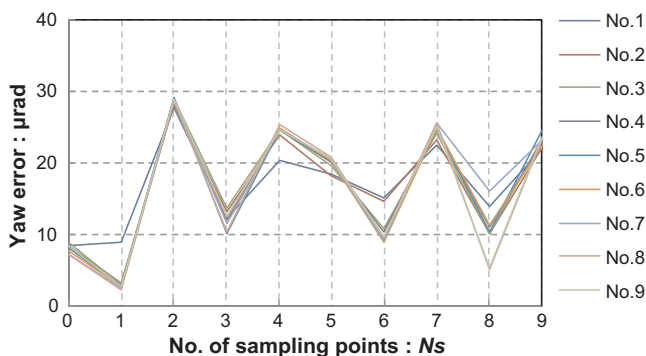


Fig. 13. Yaw error of X stage.

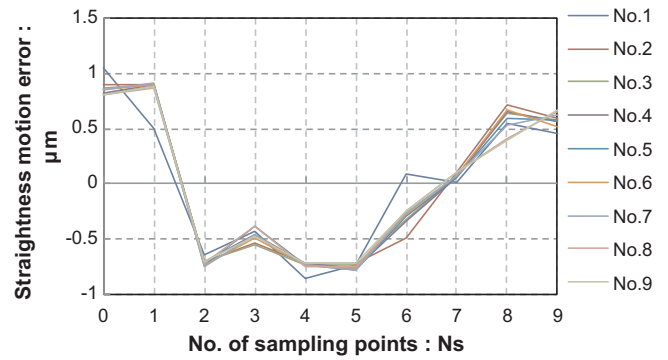


Fig. 14. Straightness motion error of X stage.

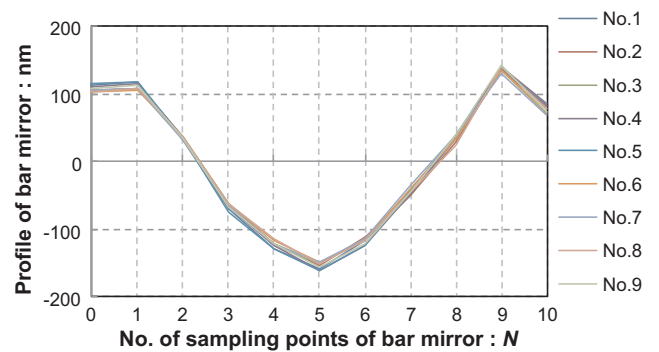


Fig. 15. Reference bar mirror profile.

erence bar mirror profiles are shown in Fig. 15, and the repeatability is good.

If we consider the standard deviation of each sensor as $\sigma_1 = \sigma_2 = 4$ nm, and $\sigma_a = 0.23 \mu\text{rad}$, the simulation results of the uncertainty of the multi-probe measurement method in the pre-experiment (2σ) is approximately 10 nm, as shown in Fig. 16. The two times standard deviations (95%) of the reference bar mirror profile are obtained by conducting the pre-experiment nine times. The curve of the two times standard deviation values of the reference bar mirror profile approximately fits 2σ range (Fig. 16). We can conclude that the multi-probe measurement method performs well while measuring the reference bar mirror profile with a small deviation of 10 nm.

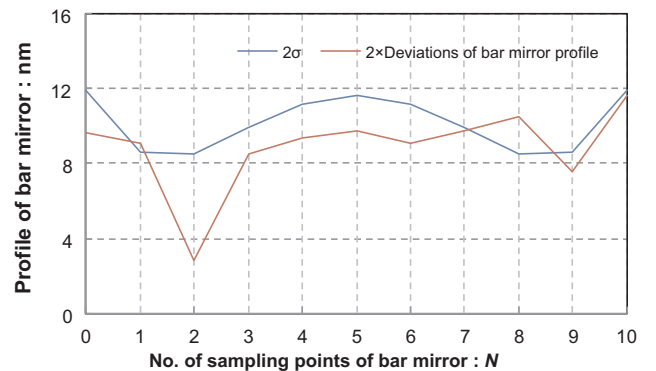


Fig. 16. Comparison of the two times standard deviation of the reference bar mirror profile with simulation results of the uncertainty of multi-probe measurement method.

7. Conclusions

We have devised a multi-probe measurement method to calibrate the motion errors of the M-CMM. We used one autocollimator and two laser interferometers to measure the yaw and the straightness motion error of the moving stage; the reference bar mirror profile could be calculated simultaneously. From the simulation results and the pre-experiment results, the conclusions of this study can be summarized as follows:

- (1) The simulation results show that the ratio of the standard deviation of the autocollimator to those of laser interferometers, $k = \sigma_a / \sigma_M$, and the number of sampling points of the reference bar mirror, N , are two important factors that affect the uncertainty value of the multi-probe measurement method.
- (2) The pre-experiment results show that the standard deviations of the laser interferometers and autocollimator are $\sigma_1 = \sigma_2 = 4 \text{ nm}$ and $\sigma_a = 0.23 \mu\text{rad}$, as shown in Figs. 11 and 12. The standard deviations of the laser interferometers in the pre-experiment are larger than the theoretical resolution value. Two main factors affect the deviation value of the laser interferometers the optical device setup and the impact from the measurement environment, such as air-refractive-index fluctuations and vibration. These factors will be considered in greater detail in our next experiment.
- (3) The horizontal measurement resolution is limited by the use of only two laser interferometers because there are only 10 sampling points in the measurement scale of 100 mm. A method using three laser interferometers and one autocollimator has been proposed to improve this disadvantage, and a new pre-experiment has been designed. We are planning to conduct the new pre-experiment in the near future.

References

- [1] Cao S, Brand U, Kleine-Besten T, Hoffmann W, Schwenke H, Bütefisch S, et al. Recent developments in dimensional metrology for microsystem components. *Microsyst Technol* 2002;8:3–6.
- [2] Vermeulen MMPA, Rosielle PCJN, Schellekens PHJ. Design of a high-precision 3D-coordinate measuring machine. *Ann CIRP* 1998;47(1):447–50.
- [3] Bos EJC, Delbressine FLM, Haitjema H. High-accuracy CMM metrology for micro systems. In: Proc. 8th int. symp. on measurement and quality control in production. Düsseldorf: VDI; 2004. p. 511–22.
- [4] Mitutoyo, UMAP Vision System, Bulletin No. 1631.
- [5] Bryan JP. The Abbe principle revisited: an updated interpretation. *Prec Eng* 1979;1:129–32.
- [6] Zhang GX. A study of the Abbe principle and Abbe error. *Ann CIRP* 1989;38:525–8.
- [7] Koning R, Flugge J, Bosse H. A method for the in situ determination of Abbe errors and their correction. *Meas Sci Technol* 2007;18:476–81.
- [8] Whitehouse DJ. Some theoretical aspects of error separation techniques in surface metrology. *J Phys E: Sci Instrum* 1976;9:531–6.
- [9] Evans CJ, Hocken RJ, Estler WT. Self-calibration: reversal, redundancy, error separation, and 'absolute testing'. *Ann CIRP* 1996;45(2):617–34.
- [10] Gao W, Kiyono S. High accuracy profile measurement of a machined surface by the combined method. *Measurement* 1996;19:55–64.
- [11] Gao W, Yokoyama J, Kojima H, Kiyono S. Precision measurement of cylinder straightness using a scanning multi-probe system. *Prec Eng* 2002;26:279–88.
- [12] Weingärtner I, Elster C. System of four distance sensors for high accuracy measurement of topography. *Prec Eng* 2004;28:164–70.
- [13] Elster C, Weingärtner I, Schulz M. Coupled distance sensor systems for high-accuracy topography measurement: accounting for scanning stage and systematic sensor errors. *Prec Eng* 2006;30:32–8.
- [14] Liu SJ, Watanabe K, Chen X, Takahashi S, Takamasu K. Profile measurement of a wide-area resist surface using a multi-ball cantilever system. *Prec Eng* 2009;33:50–5.
- [15] Yang P, Shibata S, Takahashi S, Takamasu K, Sato O, Osawa S, et al. Development of high precision coordinate measuring machine (CMM) (1st report, evaluation method of XY stage). In: JSPE autumn conference. 2009. p. 725–6.
- [16] Yang P, Shibata S, Takahashi S, Takamasu K, Sato O, Osawa S, et al. Development of high precision coordinate measuring machine (CMM) (2nd report, pre-experiment of multi-probe method for evaluating the XY stage). In: JSPE spring conference. 2010. p. 377–8.